Journal of Non-Crystalline Solids 492 (2018) 94–101

Contents lists available at ScienceDirect

Journal of Non-Crystalline Solids

journal homepage: www.elsevier.com/locate/jnoncrysol

Lateral hardness and the scratch resistance of glasses in the Na_2O-CaO-SiO_2 system

Guilherme N.B.M. de Macedo[a], Shigeki Sawamura[a,b], Lothar Wondraczek[a,*]

[a] Otto Schott Institute of Materials Research, University of Jena, Fraunhoferstrasse 6, D-07743 Jena, Germany
[b] Asahi Glass Co., Ltd., 1150 Hazawa-cho, Kanagawa-ku, Yokohama-shi, Kanagawa 221-8755, Japan

ARTICLE INFO

Keywords:
Scratching
Scratch hardness
Soda lime silicate
Defect resistance

ABSTRACT

We report on the lateral hardness of glasses from the Na_2O-CaO-SiO_2 (NCS) system, including CS and NS binaries. Quantitative data are provided on the work of lateral deformation, obtained through instrumented indentation by monitoring the lateral force as a function of normal load. Experiments were conducted in the regime of elastic-plastic deformation, that is, in the absence of microscopic cracking for normal loads of 50–70 mN. The scratch hardness is determined from the work of deformation per deformed volume. Parallel observations of the elastic properties are undertaken so as to reference scratching data to glass composition and structure. We find that structural densification and high rigidity favor higher scratch hardness. For the considered range of chemical compositions, the scratch hardness exhibits an approximately linear correlation with bulk modulus and packing density. It increases in the direction of compositions with higher content of CaO, and decreases with the content of Na_2O. Furthermore, we find a strongly linear correlation between scratch hardness and the deviation of experimental compressibility from the mean-field estimate of the Makishima-Mackenzie model. This points to the importance of intermediate-range structural heterogeneity in the scratching process.

1. Introduction

The most important glasses for daily use as well as for technical application are from the soda lime silicate (NCS) chemical system, representing approximately 90% of the global glass production [1]. Like all other oxide glasses, also NCS glasses promise intriguingly high intrinsic strength [2]. Because of their inherent brittleness and the notorious occurrence of stress-amplification at surface defects, on the other hand, the usable strength of real-world glass products remains at a small fraction of this. It is common consensus that understanding the initiation of surface defects holds the key for glasses with improved mechanical properties.

However, while the mechanical properties of NCS glasses are widely studied [3–11], the early stages of surface deformation which precede the occurrence of microscopic flaws and fracture are still unclear. In particular, this concerns the occurrence of plastic deformation, shear and structural compaction upon initial surface contact. From mild handling to forceful scratching, such contact situations occur at any stage of the product's lifetime, where they may – in concert with humidity adsorption and stress corrosion – induce surface flaws to further reduce usable strength [12,13].

Recent efforts to understand the defect resistance of glasses aim primarily for new glass compositions with improved ability to locally dissipate mechanical energy (for example, [14,15]). This mostly draws on micro-indentation testing [16–19], where it is observed that the indentation response contains contributions of elastic deformation, structural compaction and shear. One must also note, however, that laboratory testing by conventional micro-indentation often presents an idealized state. The typical indentation depth is not always representative for real-world contact situations, which may be significantly less harsh. In particular, scratch damage cannot be predicted through normal indentation experiments [20,21].

While recent experimental progress allows for quantitative testing of lateral hardness [20], the scratch resistance is a mostly phenomenological parameter [22–25]. Scratch damage occurs over the regimes of plastic deformation, radial cracking, median/lateral cracking and chipping, and microabrasion, in order of increasing normal load and dependent on scratch speed and applied shear-stress [7,26–29]. Analyzing the vertical contact area during a lateral indentation test as a function of normal load, Yoshida et al. [30] introduced the term *scratch hardness*. Thereby, the scratch hardness reflects the resistance of a material to plastic deformation during quasi-static lateral indentation [20].

We now quantitatively analyze the lateral (scratch) hardness of

* Corresponding author.
E-mail address: lothar.wondraczek@uni-jena.de (L. Wondraczek).

https://doi.org/10.1016/j.jnoncrysol.2018.04.022
Received 9 March 2018; Received in revised form 9 April 2018; Accepted 11 April 2018
Available online 24 April 2018

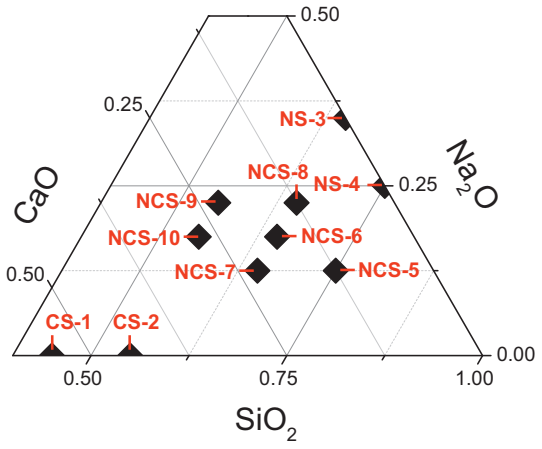

Fig. 1. Location of the present glasses in the Na_2O-CaO-SiO_2 ternary.

glasses from the archetype NCS system. We do this by directly determining the work of lateral deformation as a function of deformed volume, in the plastic regime of scratching. Through relation of the obtained data to elastic properties and conventional hardness studies, we further elucidate the physical origin of scratch resistance as a characteristic measure of mechanical performance.

2. Materials and methods

2.1. Glass melting

Glasses were produced from batches of analytical-grade SiO_2, Na_2CO_3 and $CaCO_3$. Compositions were chosen from within the ternary of Na_2O-CaO-SiO_2 (NCS), and from the two binaries of Na_2O-SiO_2 (NS) and CaO-SiO_2 (CS). Compositions were selected so that the nominal ratio of non-bridging oxygen species (NBO) over bridging-oxygen species (BO) varies within approximately 1.5 to 0.2, see also Fig. 1. Powder batches of 100 g were homogenized and melted in Pt crucibles, in a muffle furnace at temperatures ranging from 1200 to 1550 °C. A first melting step was conducted for 3 h, after which the glass was quenched in water, followed by a second melting step using the dried glass frit for another 3 h. From the frits the glass transition temperature (T_g) was obtained using a differential scanning calorimeter (DSC, STA 449 F1 Jupiter, Netzsch). The analyses were performed in a platinum crucible and applying a heating rate of 10 K/min. The applied experimental melting temperatures (T_m) for each glass are indicated in Table 1. After the second melting step, melts were cast onto a copper block and pressed with a brass plate to avoid crystallization. The samples were subsequently transferred to a muffle furnace, pre-heated to a temperature of approximately 0.95 of the corresponding T_g and annealed for 1 h. Final cooling to room temperature was done at the furnace rate of < 2 K/min. Obtained glasses were cut into slides with a thickness of 1 to 2 mm and polished on both sides, using fine-grained CeO_2 as polishing agent. Details of the glass compositions can be found in Table 1. Densities were evaluated via the Archimedes method.

2.2. Elastic properties and Vickers hardness

Elastic properties were evaluated through ultrasonic analysis. In order to determine the transversal and longitudinal speed of sound (c_t and c_l), the thickness of each sample was initially measured with a precision of ± 2.5 µm using a micrometer screw. An echometer (Echometer 1077, Karl Deutsch) with a transducer operating at frequencies of 8 to 12 MHz was subsequently employed to determine the propagation times of the transversal and longitudinal sound waves, from which c_t and c_l were calculated. Then, bulk modulus *(K)*, elastic modulus *(E)* and Poisson's ratio *(ν)* were calculated using Eqs. 1–3 [31],

Table 1
Nominal composition and properties of the studied glasses. NBO and BO (denoting relative number of non-bridging and bridging oxygen species) were calculated according to Ref. [37].

	CS-1	CS-2	NS-3	NS-4	NCS-5	NCS-6	NCS-7	NCS-8	NCS-9	NCS-10
CaO (mol%)	55	45	0	0	12.5	17.5	22.5	12.5	22.5	27.5
Na_2O (mol%)	0	0	35	25	12.5	17.5	12.5	22.5	22.5	17.5
SiO_2 (mol%)	45	55	65	75	75	65	65	65	55	55
T_m (°C)	1550	1550	1200	1350	1350	1350	1350	1350	1350	1500
T_g (°C)	785[c]	769[c]	470	490[d]	588	623	562	564	596	591
NBO	2.44	1.64	1.08	0.67	0.67	1.08	1.08	1.08	1.64	1.64
BO	1.56	2.36	2.92	3.33	3.33	2.92	2.92	2.92	2.36	2.36
E_{IT}[a] (GPa)	98.8	92.1	60.8	60.5	79	87.1	84.9	79.8	87.3	91.4
E[b] (GPa)	89.0 ± 1.7	86.0 ± 1.7	–	62.6 ± 1.4	77.9 ± 0.7	80.0 ± 1.3	77.7 ± 1.3	75.4 ± 0.7	80.6 ± 1.4	85.0 ± 1.0
K[b] (GPa)	71.9 ± 1.4	61.4 ± 1.2	41.2 ± 1.2	38.9 ± 0.5	45.1 ± 0.8	51.6 ± 0.9	52.8 ± 0.9	48.4 ± 0.5	54.7 ± 0.9	55.2 ± 0.6
ν[b]	0.294 ± 0.006	0.267 ± 0.005	0.254	0.241	0.213 ± 0.002	0.242 ± 0.004	0.255 ± 0.004	0.241 ± 0.002	0.254 ± 0.004	0.244 ± 0.003
H_{IT} (GPa)	8.23	8.04	5.05	5.24	6.98	7.76	7.75	7.08	7.6	7.59
H_V (GPa)	6.38	6.13	–	–	5.29	6	6.04	5.41	5.92	5.95
H_s (GPa)	9.81	8.83	–	5.47	6.23	7.64	7.71	6.72	7.99	8.07
H_V/H_{IT}	1.2	1.1	–	1	0.9	1	1	0.95	1.05	1.06
C_g	0.516	0.514	0.493	0.489	0.497	0.509	0.503	0.502	0.508	0.51
V_f (cm^3/mol)	20.339	21.121	24.395	24.854	23.896	22.839	22.877	23.389	22.389	22.09
ρ (g/cm^3)	2.843	2.757	2.49	2.436	2.5023	2.613	2.596	2.565	2.661	2.683

[a] Determined by nanoindentation.
[b] Determined by echometry.
[c] From reference [38].
[d] From reference [5].